Research Article **SRR (2021) 14:123**

Scientific Research and Reviews
(ISSN:2638-3500)

Innovative testing technique of rock stress wave propagation

Qing-yu Song[1*], Rui Zhang[2]

[1]School of Earth Science and Engineering, Hebei University of Engineering, Handan, Hebei 056038, China.
[2]School of Architectural and Surveying Engineering, Jiangxi University of Science and Technology, Ganzhou, Jiangxi 341000, China.

ABSTRACT

Inadequacy of rock mechanics chamber test devices and test systems that cannot accurately simulate gradient static stresses on specimens, this paper presented an innovative testing technique, which relates to the stress wave propagation of rock subjected gradient static stress. The method involves modification of a split Hopkinson pressure bar, such that the test specimen is subjected to gradient static stress and axial impact loading. The device has the features of simple loading and multiple static stress gradients, which verifies the feasibility of stress wave propagation test of red sandstone specimens under linear gradient static stress and conducts stress wave propagation test of red sandstone specimens under linear gradient static stress. Tests on red sandstone specimens with different static stress gradients show that the stress wave propagation of the specimens under gradient static stress is different with their corresponding homogeneous static stress state. The attenuation coefficients of stress waves are different under different conditions, and loading gradient static stress can accelerate the attenuation process. The results of this study will be useful for the analysis of stress wave propagation in deep engineering blasting and the stability analysis of adjacent structures.

Keywords: Stress wave propagation; Rock; SHPB system; Gradient static stress

***Correspondence to Author:**
Qing-yu Song
School of Earth Science and Engineering, Hebei University of Engineering, Handan, Hebei 056038, China.

How to cite this article:
Qing-yu Song, Rui Zhang. Innovative testing technique of rock stress wave propagation. Scientific Research and Reviews, 2021; 14:123

eSciPub LLC, Houston, TX USA.
Website: http://escipub.com/

List of Symbols

$F_f(x)$ The static friction force of friction per unit length

l The length of specimen

f_s The friction force coefficient between specimen and external components

$F_N(x)$ The normal pressure cating on the unit length of specimen

σ The axial static stress

x the cross section

A cross-sectional area of specimen

F_f a constant value, the static stress on the cross-section of the specimen presents a linear gradient distribution. Otherwise, it is non-linear gradient distribution.

F_p Pretightening force loading on bolt

M Torque applied by torque wrench

k_0 Coefficient about torque

d Bolt diameter

W_I Energy of incident wave of elastic rod

W_R Energy of reflected wave from elastic rod

W_G Energy on steel plate

W_S Energy on specimen

E elastic modulus

C longitudinal wave velocity

ρ density

A cross-sectional area

$\varepsilon_I(t)$ Strain Wave of Elastic Rod Incident Waves

$\varepsilon_R(t)$ Strain waves reflected by elastic rods

$\varepsilon_G(t)$ Strain waves of incident waves on steel plates

$\varepsilon_S(t)$ Strain waves of incident waves on specimens

W_J Energy dissipated by the stress wave in the process of propagation of the test piece and rubber

ε_I The amplitude of the incident wave

R^2 correlation coefficient

$\varepsilon(t)$ The stress wave amplitude at any moment t

α_t The time decay coefficien

β_t Represents the stress wave amplitude at t=0, which is the amplitude time response strength.

1. Introduction

Blast (impact load), which is uniquely characterized by the rapid acts on specimens in loads, has recently become a topic of increased research in the fields of rock mechanics and rock engineering. Chi et al. (2019) studied the rupture of granite cubes (400×400 and 400mm^3) under blast loading. Based on data from a large number of in situ measurements from China and Taiwan a new relationship, based upon asigmoid function, is by proposed (Hoek et al. 2006). This study investigates the effect of rock

shape on the variability of the impact breakage test conducted on impact load cells by Bonfils (2017). Raina (2019) has discussed the basis of pre-splitting opposite dominant variables afecting performance.

Generally, Blast (impact load) changes dynamic motion parameters in a very short time, such as milliseconds, microseconds, even nanoseconds. Under such dynamic loads, the microelement is in a dynamic process that changes rapidly with time. Not statically, but dynamically apply to the above conditions. Extensive studies have been conducted to simulate similar experimental conditions in lab (Davies 1948; Whittles et al. 2006). Hopkinson (1914) and Kolsky (1949) who participate in created split-Hopkinson pressure bar (SHPB), making contribution to the development of petrodynamics.

Currently, there are various setups and techniques in use for the SHPB, but the underlying principles for the test and measurement are the same. One of the schematic diagrams of a SHPB setup is shown in Fig.1, which could provide no static load to specimen. Specimen, which applied dynamic loads based SHPB setup showed by Figure 1, exhibits different mechanical properties at high strain rates rather than specimen which applied static loads (Yi et al. 2006; Armstrong 2008). Creatively, Xibing Li improved SHPB setup, which puts forward innovative testing technique of rock subjected to coupled static and dynamic loads (Li et al. 2008). Extensive studies have been applied to investigate relationship between load and stress wave propagation based on modified SHPB (Tan et al. 2019; Dai et al. 2010; Zhu et al. 2012 and Wu et al. 2019).

In engineering practice, the magnitude of static stress on each cross section is not equal for many structural members in normal operation, which is called gradient static stress. If the cross-sectional area of large-volume concrete such as piers of large bridges is equal everywhere, the static stress of each cross-section is different along the axial direction from top to bottom and takes the form of isogradient. During the excavation of deep underground caverns, due to the influence of stress redistribution and other factors, the rock mass within a certain range along the excavation face is in a state of non-equal gradient stress (Su et al. 2017).

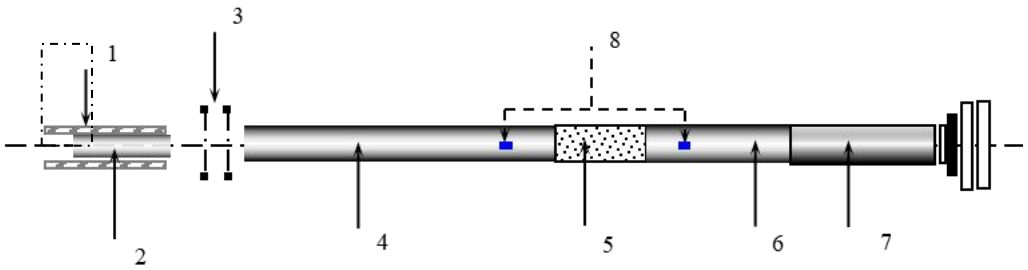

Fig.1 The schematic diagram of a SHPB setup:1—Emission cavity; 2—Striker; 3—Transient recorder; 4—Input bar; 5—Specimen; 6—Output bar; 7—Absorption bar; 8—Strain gauge.

Research on stress wave propagation with gradient static loads is scarce, even though these stress states commonly occur deep underground. Thus, it is necessary for us to investigate the behavior of rocks under such conditions. This paper presents an innovative labora-

tory testing technique to simulate the stress wave propagation of rock with gradient static loading. Test results are provided and the findings are discussed.

2. Equipment and test methods

A new testing system for researching stress wave propagation with gradient static loads has been successfully constructed and commissioned. Diagrammatic details of the new test system are shown in Fig. 3. Broadly speaking, the system consists of the striker launcher, stress wave transmission component, gradient pre-compression stress inducer and data processing unit. The striker launching setup comprises the striker, gas tank, pressure vessel, gas switches and outlet valves. In order to produce half-sine waveform, a double tapered shape striker, which can reduce wave disperion effcets and eliminate wave oscillation, is adopted (Lok et al. 2002; Li et al. 2000). The parameters of the needle selected in this paper are the same as Li et al. (2005). The stress wave transmission component is made up of long elastic bar, which are 50mm in diamter and 1.5m in length. As shown in Fig. 3, the elastic bar is on the left side of specimen. The gradient pre-compression stress inducer is shown in Fig.4. Strain gauges are glued on the surface of the middle of specimen to measure strain histories induced by the stress waves propagating along the elastic bar. The amplitude of incident impact loading depends on the speed of striker, which can be changed by means of changing air pressure in the pressure vessel and the position of the striker. The data processing unit is made up of a CS-1D super dynamic strain meter, a DL750 ScopeCorder digital oscilloscope (Yokogawa) and a personal computer with integrated data processing software.

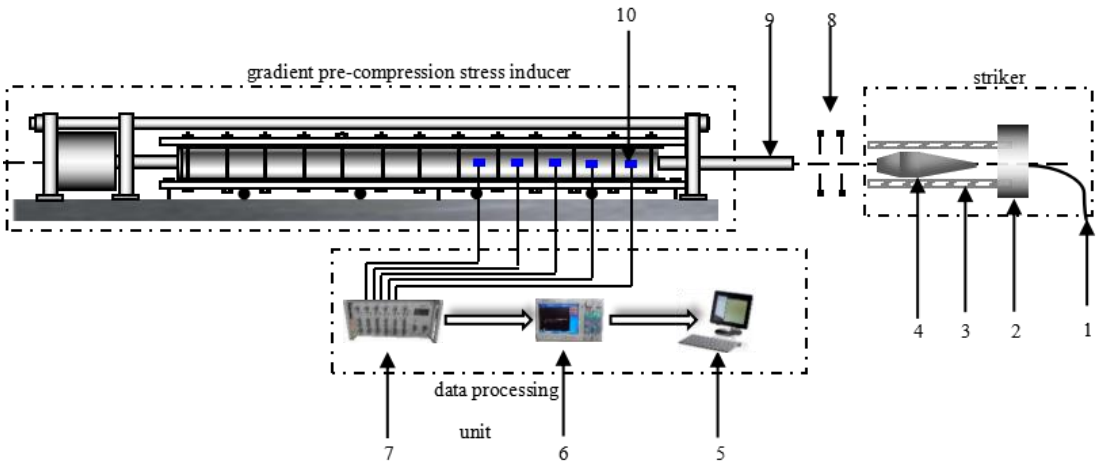

Fig. 2 Experimental device about stress wave propagation under gradient static stress: 1—HP Nitrogen; 2—HP gas vessel; 3—Emission cavity; 4—Striker; 5—computer; 6—Digital oscilloscope; 7—Super dynamic strain meter;8—Transient recorder; 9—Elastic bar/Stress wave transmission component;10—Strain gauge.

Fig. 2 is an experimental device about stress wave propagation under gradient static stress. Gradient pre-compression stress inducer is shown in Fig.4. In preparation, in order to apply normal loads to specimen, pretightening force, which is transformed by torque, transforms to

apply normal loads to specimen by steel. Axial pressure loading unit then applies axial loads to specimen. The magnitude of axial load applied to the specimen should be considered in order to reach the critical state of the specimen, the stationary state of relative sliding. Once the setup is ready, the striker is launched. On impact, an incident wave is developed and it propagates along the elastic bars and specimens. Strain gauges, distributing on the front and rear sides of the specimen, capture reflected and transmitted signals and display on the oscilloscope. Then, the signals are processed by personal computer to obtain stress wave amplitude, wave velocity and other information.

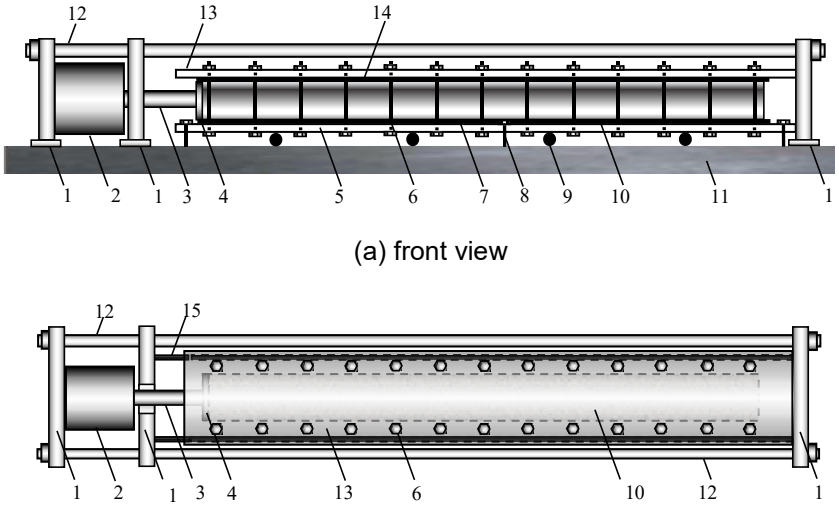

(a) front view

(b) top view

Fig.3 Experimental device for applying gradient static stress to specimens (Jin et al.2020)

1—thin baffle screen; 2—pressure loading unit (together with 1 and 12 to form the axial pre-compression stress setup); 3—loading rod; 4—steel; 5—lower steel plate; 6—loaded bolt; 7—lower rubber; 8—stable bolt; 9—roller; 10—specimen; 11—base; 12—steel frame; 13—top steel plate; 14—top rubber; 15—T-slot.

Experimental device for applying gradient static stress to specimens is made up of thin baffle screen, two steels with bolt holes, torque wrench, bolts, rubber, roller and pressure loading unit. Thin baffle screen, placed on a horizontal plane, provides a horizontal experimental platform for superstructure. The size of the steel is 1700mm ×215mm×10mm. The spacings of bolt holes, setting at equal spacing, are set up 135 mm in experiments by considered carefully and discreetly. The longer the spacing is, the weaker the accuracy is. Otherwise, the more complex the operability is. Thickness of rubber is 3~5mm. Bolts, placed in bolt holes, are applied tightening torque by torque wrench, which is converted into the bolt pre-tightening force. Rubber and steels, placed the upper and lower sides of the specimen respectively, apply normal load by pre-tightening force of bolts. The right side of the steel is in close contact with thin baffle screen, which spacing 3~5cm with specimen. After loading normal loadings, specimen is loaded axial loads by pressure loading unit. Under the action of axial load, the specimen has a relative sliding tendency because of the spacings between specimen and thin baffle

screen. The bigger axial load is, the more obvious tendency is. With the increase of axial load, specimen will be in a critical state, the stationary state of relative sliding. At this point, the friction between the specimen and the rubber is the maximum static friction force, and the specimen bears the gradient static stress. Stable bolts are set to hold the steel in place. Rollers allow the superstructure to move freely horizontally.

3. Testing technique simulating gradient static loads

This part will illustrate the feasibility of applying gradient static stress to the specimen from theoretical analysis to experimental verification.

3.1 Theoretical validation

A number of studies have been conducted to simulate the stress states of gradient static loads from different perspectives(Wang et al. 2014; Jin et al. 2016). However, the exact static gradient cannot be obtained from studies although other meaningful data were extracted. In addition, a large static stress gradient cannot be applied. The gradient static stress provided by the device to the specimen is provided by friction force, which derives from relative sliding between specimen and external medium.

As shown in Fig.4, we applied axial load *F* to the specimen, which have been applied normal load F_N. When the specimen is applied axial load *F*, there is a relative sliding trend between the specimen and external components, with static friction force F_f, which has opposite direction with axial load *F* appearing. With the increases to a certain critical value of *F*, all parts of the specimen section bear the same maximum static friction force named critical state, the static state of relative sliding between specimen and external components. The axial force on each cross section is different, which means the axial static stress on the cross section changes in a gradient form along the axis(Jin et al.2020).

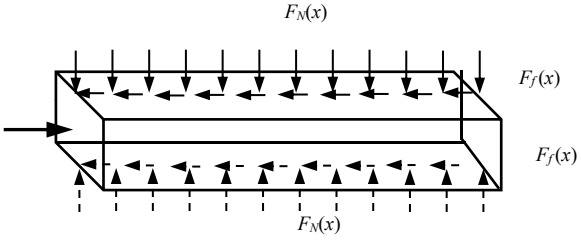

Fig.4 Schematic diagram for applying gradient static stress to specimens

The axial concentrated force *F* is equal to the static friction force F_f under critical state,

$$F = 2\int_0^l F_f(x)dx \tag{1}$$

Where $F_f(x)$ is the static friction force of friction per unit length, *l* is the length of specimen. According to Coulomb's Law, the friction force on the unit length of the specimen is written as

$$F_f = f_s \times F_N(x) \tag{2}$$

Where f_s is the friction force coefficient between specimen and external components. $F_N(x)$ is the normal pressure cating on the unit length of specimen.

When $F_f(x)$ is a constant value along the length direction of specimen, then

$$F=2F_f l \tag{3}$$

The axial static stress σ on the cross section x away from the right end face is

$$\sigma=\frac{2F_f \bullet x}{A} \tag{4}$$

Where A is cross-sectional area of specimen. When F_f is a constant value, the static stress on the cross-section of the specimen presents a linear gradient distribution. Otherwise, it is non-linear gradient distribution.

3.2 Feasibility of the constructed system

In this paper, the feasibility and application of the device are investigated under the condition that the specimen is subjected to equal gradient. The related research on the specimen under the condition of non-equal gradient stress is described in other papers. The premise of the feasibility of the experimental device is applying precise gradient static stress to the specimen. This part mainly includes accuracy of applying gradient static stress to specimens and effect of superstructure on stress wave propagation in specimen.

3.2.1 Applying precise gradient static stress to the specimen

In order to check the accuracy of the designed system, 10N·m, 15N·m, 20N·m and 25N·m torque were used to conduct trial tests, with 304 stainless steel of 1317mm× 60mm× 60mm. Parameters of specimens in trial tests are shown in Table. 1. In order to apply normal loads to specimen, torque wrench is used to apply torque to bolts. Pretightening force, which is transformed by torque, transforms to apply normal loads to specimen by steel. The relationship between torque and pretightening force can be written as (Huang et al. 2015).

$$F_P=\frac{M}{k_0\times d} \tag{5}$$

Where F_p is pretightening force loading on bolt, M is torque applied by torque wrench, k_0 is coefficient about torque,d is bolt diameter. In this paper, k_0=0.19, d=14mm.

After loading normal loadings, specimen is loaded axial loads by pressure loading unit till to the critical state. The method to determine the critical state, in different conditions, is described as follows: The manual hydraulic device slowly injection hydraulic oil to pressure loading unit, which applies axial loads to specimen slowly. The loading speed of the loading rod is every three seconds. Observe the relative position of the specimen and the rubber, record the readings of the oil pressure meter when the two slide relative to each other. Then repeat three times. If the error of the three is less than 0.5MPa, the average value is the axial pressure under different conditions. Stress gradient in different conditions can be written as

$$k=\frac{F}{A\bullet l} \tag{6}$$

There are 8 strain gauge setting on 304 stainless steel. The distance from the right side of the 304 stainless steel specimen is 11.7cm, 26.7cm, 41.7cm, 56.7cm, 71.7cm, 86.7cm, 101.7cm and 116.7cm respectively. The summary of theoretical data and measured data are shown in Fig. 5. The percentage of jagging in different conditions is shown in Table 2.

Table 1 Parameters of specimens in trial tests

Specimen	Size (mm)	Density (g/cm^3)	Wave velocity (m/s)	Elasticity modulus (GPa)	Poisson's ratio	compressive strength/ Strength of extension (MPa)
Red sandstone	1500×60×80	2.46	3560	15.47	0.29	96
304 stainless steel	1317×60×60	7.93	-	195	0.25	520

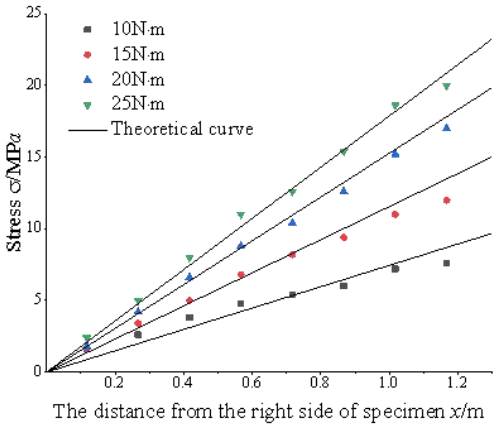

Fig. 5 The summary of theoretical data and measured data

Table 2 The percentage of jagging in different conditions

Torque (N·m)	Theoretic formula	The percentage of jagging (%)
10	$\sigma(x)=7.45x$	8.54
15	$\sigma(x)=11.55x$	5.71
20	$\sigma(x)=15.27x$	2.01
25	$\sigma(x)=17.88x$	2.36

3.2.2 Effect of superstructure on stress wave propagation in specimen

By striking the incident bar with a punch at high speed, the stress wave generated at this time produces a reflection phenomenon. Part of the incident wave is of the incident ray type and is transmitted into the specimen. The stress wave propagates inside the specimen.Total energy depends on mass and speed of striker. The same striker, which impacts in same speed, produces the same total energy. A small part spreads to the upper and lower interfaces of the test piece. The flexible medium (rubber) absorbs most of the energy transmitted to the steel. The energy on the steel can be divided into two parts, most of it spreads along steel, while a small part spreads to specimen. The presence of rubber makes the energy delivered to specimen small and negligible.

After several times of reflection of stress wave in the specimen, the stress is uniform at the contact interface between the specimen and the elastic rod. According to the principle of SHPB test, the energy of incident wave, reflected wave, steel plate and specimen can be calculated according to Liu et.al (2014) is calculated

according to the following formula:

$$W_I = \frac{A_I c_0}{E_0} \int_0^t \sigma_I^2(t)dt = E_0 A_I c_0 \int_0^t \varepsilon_I^2(t)dt \quad (7)$$

$$W_R = \frac{A_I c_0}{E_0} \int_0^t \sigma_I^2(t)dt = E_0 A_I c_0 \int_0^t \varepsilon_R^2(t)dt \quad (8)$$

$$W_G = \frac{A_G c_G}{E_G} \int_0^t \sigma_G^2(t)dt = E_G A_G c_G \int_0^t \varepsilon_G^2(t)dt \quad (9)$$

$$W_S = \frac{A_s c_s}{E_s} \int_0^t \sigma_s^2(t)dt = E_s A_s c_s \int_0^t \varepsilon_s^2(t)dt \quad (10)$$

Where, W_I, W_R, W_G, W_S are the incident wave, reflected wave, energy on the steel plate and the specimen in turn; E,*c*,*ρ*,A are the elastic modulus, longitudinal wave velocity, density and cross-sectional area of the specimen in turn; $\varepsilon_I(t)$, $\varepsilon_R(t)$, $\varepsilon_G(t)$ and $\varepsilon_S(t)$ are the strain waves of incident wave, reflected wave, incident wave on steel plate and incident wave on specimen. During the test, the energy loss between the elastic rod and the support and between the elastic rod and the specimen interface is ignored, and the energy exchange between each part of the test device and the outside world is ignored. Then the test should strictly meet the law of conservation of energy:

$$W_I - W_R = W_G + W_S + W_J \quad (11)$$

Where W_J is the energy dissipated by the stress wave in the process of propagation of the test piece and rubber. Since the distance between the strain gauge on the test piece and the right side is small, this part mainly represents the energy dissipated by the stress wave in the rubber propagation process. Fig 6 shows the distribution of stress wave energy in each part and the proportion of energy in the specimen.

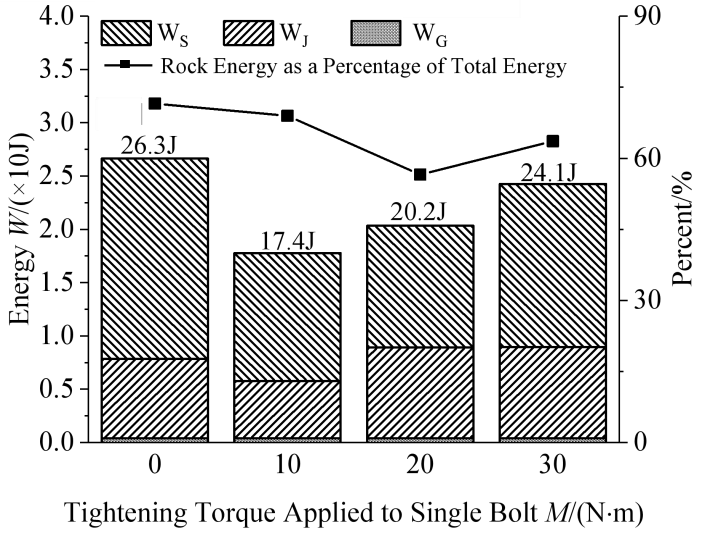

Fig.6 Stress wave energy distribution in different parts for different operating conditions

As can be seen from the figure, the proportion of energy transferred to the steel plate through the

rubber is always less than 2% of the total energy, which is negligible, and it can be considered that the superstructure has no influence on the test results.

4. Results

4.1 The effect of different working conditions on amplitude

The stress wave shape diagram under different conditions is shown in Fig. 7. In the same confining pressure, there are two types of conditions: non-axial and axial pressurized. The rock specimen is subjected to normal load only in the confining pressure with compression and without axial compression; in the confining pressure with compression and with axial compression, the rock specimen is subjected to gradient static stress.

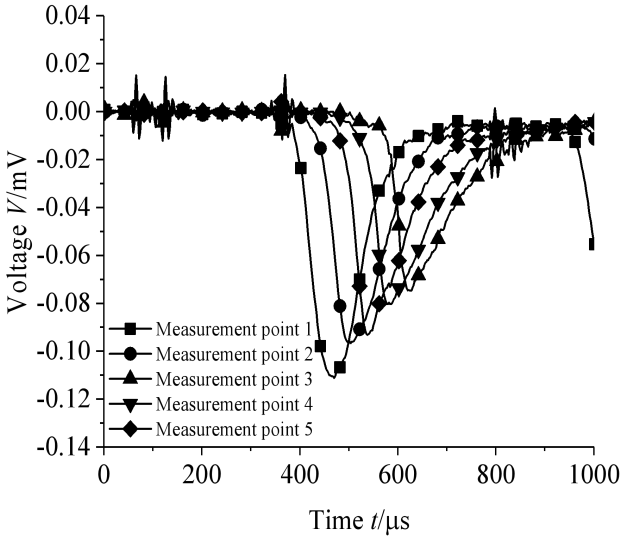

(a) confining pressure 0MPa
axial compression 0MPa

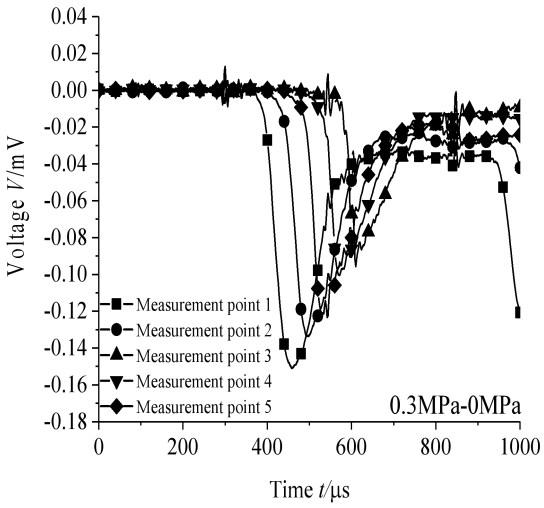

(b) confining pressure 0.30MPa
axial compression 8.83MPa

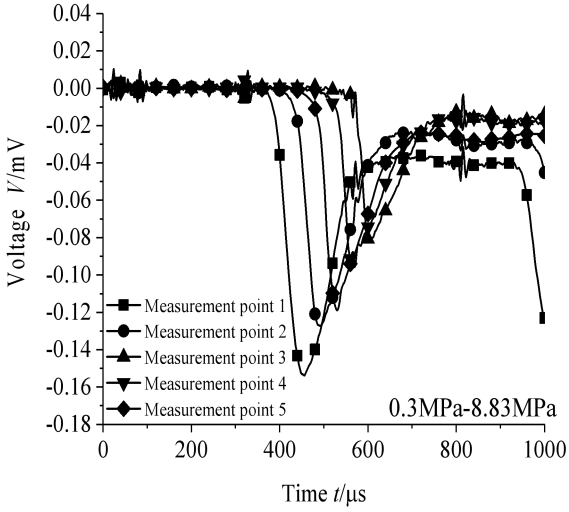

(c) confining pressure 0.30MPa
axial compression 0MPa

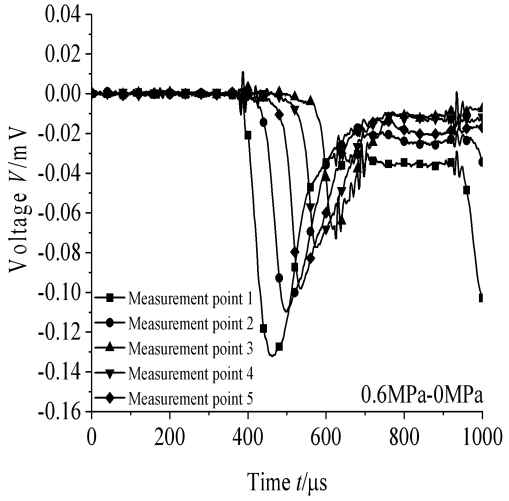

(d) confining pressure 0.60MPa
axial compression 0MPa

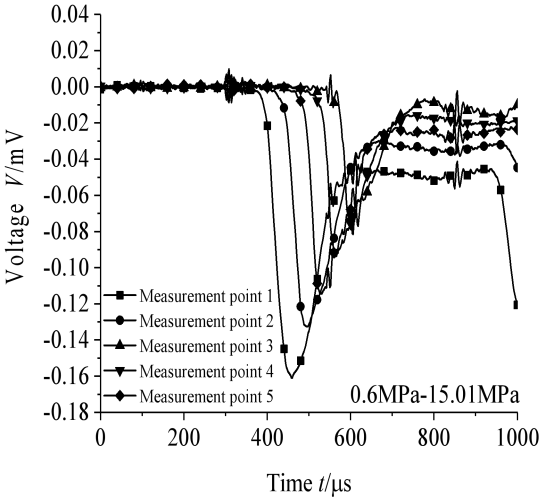

(e) confining pressure 0.60MPa
axial compression 15.01MPa

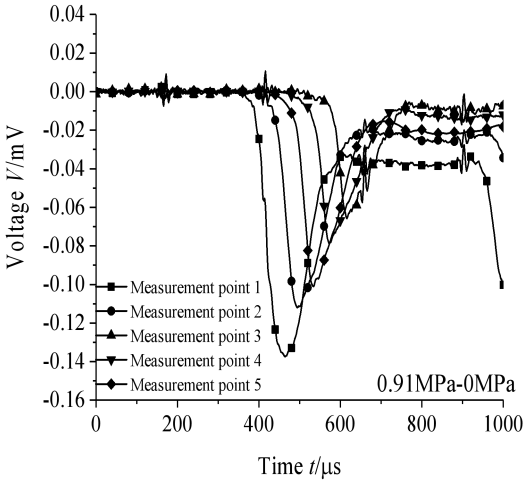

(f) confining pressure 0.91MPa
axial compression 0MPa

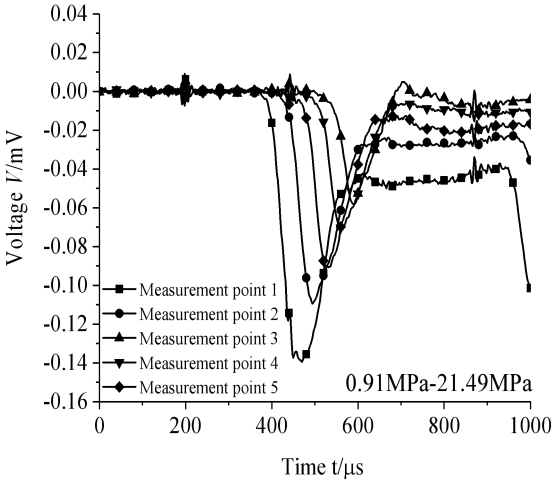

(g) confining pressure0.91MPa
axial compression21.49MPa

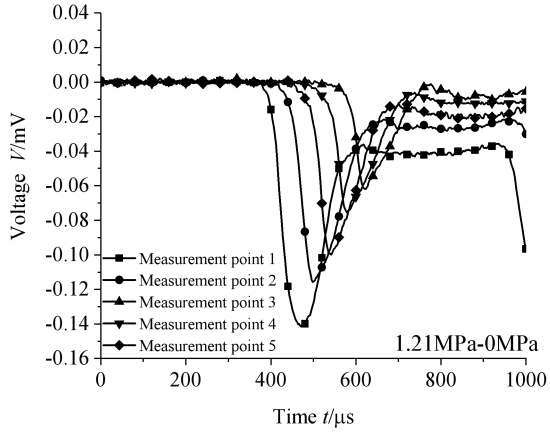

(h) confining pressure 1.21MPa
axial compression 0MPa

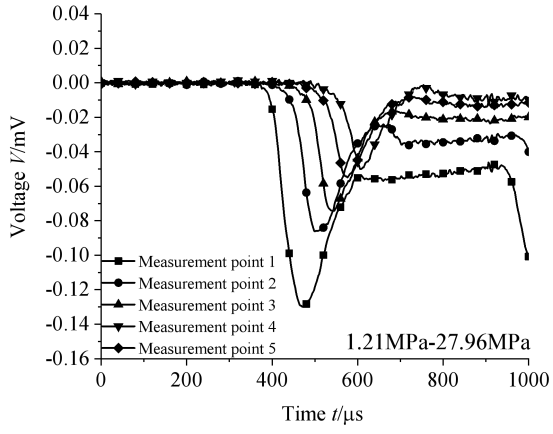

(i) confining pressure 1.21MPa
axial compression 27.96MPa

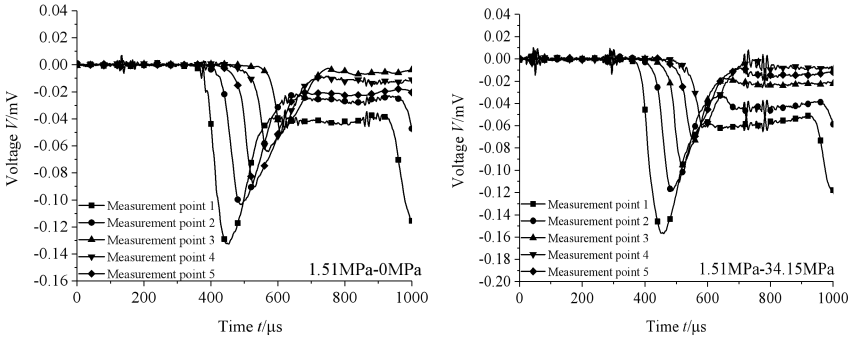

(j) confining pressure 1.51MPa axial compression 0MPa

(k) confining pressure 1.51MPa axial compression 34.15MPa

Fig. 7 The stress wave shape diagram under different conditions

As can be seen in Figure 7, under different conditions, there are obvious differences in the stress waveform, which are mainly reflected in the falling edge of the stress waveform. When the specimens are not subjected to normal loading and gradient static stress, the stress wave unloading section at each measurement point can basically return to the baseline position. Fig 7(a) Stress wave at measurement point 1 at the unloading tail (after t>800μs) strain approaches a certain value with increasing propagation time.

When the specimen is subjected to normal load and gradient static stress, respectively, the stress wave rebound changes significantly, taking the waveform at measurement point 1 in Fig 7(d) and Fig 7(e) as an example, the strain of its stress wave at the unloading tail (after t>600μs) approaches a certain value. When the specimen is subjected to normal load and gradient static stress respectively, the normal load and gradient static stress constrain the specimen's ability to recover the initial stress, resulting in the stress at each measurement point not recovering to the initial stress level.The recovery of the tail of the stress-wave unloading section when the specimen is subjected to a normal load is greater than the recovery of the tail of the stress-wave unloading section when the specimen is subjected to a gradient static stress.

4.2 Innovative testing technique of rock stress wave propagation

In the process of propagation, the stress wave amplitude gradually decreases with time and the increase of propagation distance. Figure 8 shows the time decay of the stress wave amplitude under different working conditions

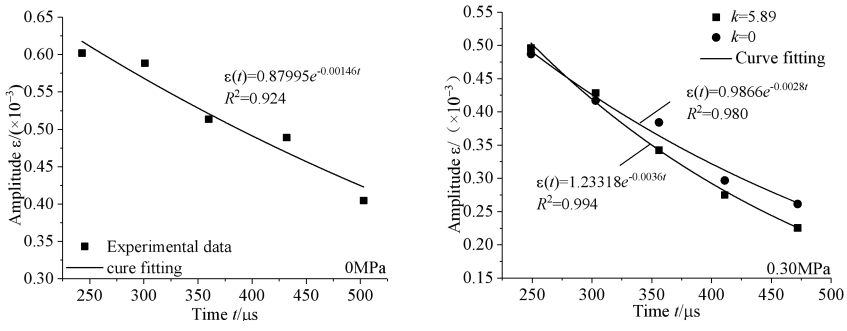

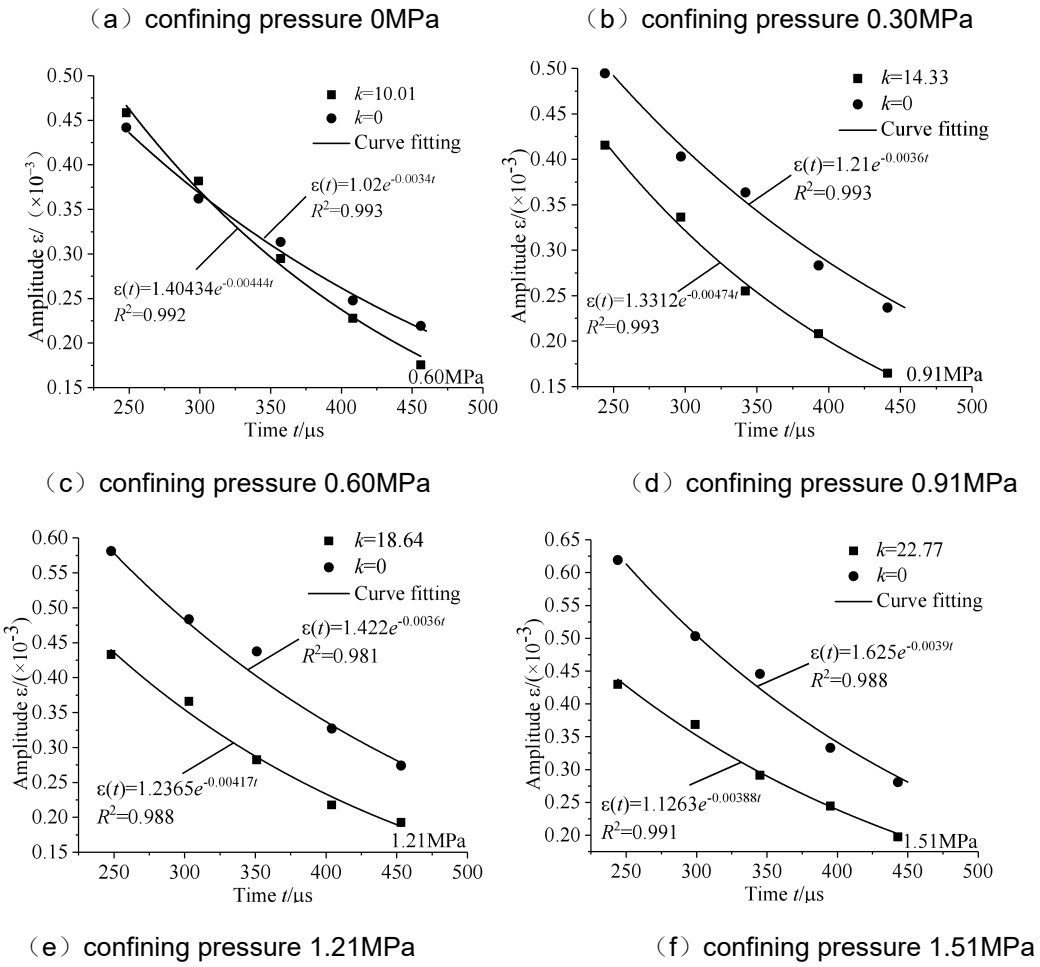

Fig. 8 Stress wave amplitude versus time

From the correlation coefficient R^2, it can be seen that the exponential function fitting has a good fitting effect, that is, the attenuation law of stress amplitude with propagation distance conforms to the exponential function. The process of propagation, the stress wave amplitude slowly decreases with time and the increase of propagation distance. Fig. 8 shows the time decay of the stress wave amplitude under different working conditions. The stress wave amplitude shows a similar variation law in different confining pressure conditions, it decreases slowly with time, but not at the same rate. In order to further investigate the effect of static stress gradient on the attenuation of stress wave propagation, the following equation is used to fit the stress wave amplitude for different working conditions：

$$\varepsilon(t) = \beta_t e^{(-\alpha_t \cdot t)} \quad (13)$$

Where $\varepsilon(t)$ is the stress wave amplitude at any moment t; α_t is the time decay coefficient, which represents the decay of amplitude with time, and the unit is μs^{-1}; β_t represents the stress wave amplitude at t=0, which is the amplitude time response strength.

Table 3 Time decay coefficients for different operating conditions

Confining pressure (MPa)	Stress gradient (MPa/m)	α_t/(μs^{-1})	correlations

0	0	0.0015	0.924
0.30	0	0.0028	0.980
	6.87	0.0036	0.994
0.60	0	0.0034	0.993
	11.78	0.0044	0.992
0.91	0	0.0036	0.993
	15.31	0.0047	0.993
1.21	0	0.0036	0.981
	19.23	0.0042	0.988
1.51	0	0.0039	0.988
	22.57	0.0039	0.991

In the same confining pressure condition, the axial stress is applied to the loaded specimen to achieve the effect of gradient static stress on the specimen. The stress wave time decay coefficient increases in the presence of the stress gradient condition, which is mainly caused by the decrease of pore space and the increase of particle contact stiffness under the axial stress. The attenuation coefficient is related to the pore fluid type, pore geometry and the structural position of the rock (Wang et al. 1988; Fan et al. 2009).

In summary, the device can be used to study stress wave propagation tests under gradient static stress.

5. Conclution

Faced on the practical solutions, where specimens are loaded formal gradient static stress and noformal gradient static stress, the device of loading gradient static stress for rock specimen is produced. The paper measures the treth of device, the conclusions are listed as follows:

1. Experimental device for applying gradient static stress to specimens is made up of thin baffle screen, two steels with bolt holes, torque wrench, bolts, rubber, roller and pressure loading unit. During loading different loads to bolt hole, formal gradient static stress and un-formal gradient static stress are applied to specimen.

2. The study of rock stress wave propagation is able to carry on by the experimental device. The attenuation coefficient of stress wave is different under different conditions. Loading gradient static stress can accelerate attenuation process.

References

[1] Chi L Y, Zhang ZX, Aalberg A, et al. Fracture processes in granite blocks under blast loading. Rock mechanics and rock engineering, 2019, 52(3): 853-868..

[2] Hoek E, Diederichs MS. Empirical estimation of rock mass modulus. International Journal of Rock Mechanics and Mining Sciences, 2006, 43(2):203-215.

[3] Bonfils B. Quantifying of impact breakage of cylindrical rock particles on an impact load cell. International Journal of Mineral Processing, 2017, 161:1-6..

[4] Raina AK. Influence of joint conditions and blast design on pre-split blasting using response surface analysis. Rock Mechanics and Rock Engineering, 2019, 52(10): 4057-4070.

[5] Hopkinson B. X. A method of measuring the pressure produced in the detonation of high, explosives or by the impact of bullets. Philosophical Transactions of the Royal Society of London. Series A, Containing Papers of a Mathematical or Physical Character, 1914, 213 (497-508): 437-456..

[6] Kolsky H. An investigation of the mechanical properties of materials at very high rates of

loading. Proceedings of the physical society. Section B, 1949, 62(11): 676..

[7] Davies RM. A Critical Study of the Hopkinson Pressure Bar. Philosophical Transactions of the Royal Society of London. Series A, Mathematical and Physical Sciences, 1948, 240(821): 375-457.

[8] Whittles DN, Kingman S, Lowndes I, et al. Laboratory and numerical investigation into the characteristics of rock fragmentation. Miner Eng, 2006, 19(14):1418–29.

[9] Yi J, Boyce MC, Lee G F, et al. Large deformation rate-dependent stress–strain behavior of polyurea and polyurethanes. Polymer, 2006, 47(1):319-329.

[10] Armstrong, W. High strain rate properties of metals and alloys.International Materials Reviews, 2008, 53(3):105-128.

[11] Li X, Zhou Z, Lok TS, et al. Innovative testing technique of rock subjected to coupled static and dynamic loads. International Journal of Rock Mechanics and Mining Sciences, 2008, 45(5): 739-748.

[12] Tan Y, Yu X, Elmo D, et al. Experimental study on dynamic mechanical property of cemented tailings backfill under SHPB impact loading. International Journal of Minerals, Metallurgy, and Materials, 2019, 26(4): 404-416..

[13] Dai F, Huang S, Xia K, et al. Some fundamental issues in dynamic compression and tension tests of rocks using split Hopkinson pressure bar. Rock mechanics and rock engineering, 2010, 43(6):657-666..

[14] Zhu WC, Bai Y, Li XB, et al. Numerical simulation on rock failure under combined static and dynamic loading during SHPB tests. International Journal of Impact Engineering, 2012, 49: 142-157.

[15] Wu Q, Li X, Weng L, et al. Experimental investigation of the dynamic response of prestressed rockbolt by using an SHPB-based rockbolt test system. Tunnelling and Underground Space Technology, 2019, 93: 103088..

[16] Su G, Zhai S, Jiang J, et al. Influence of radial stress gradient on strainbursts: an experimental study. Rock Mechanics and Rock Engineering, 2017, 50(10): 2659-2676.

[17] Lok TS, Li XB, Liu D, et al. Testing and response of large diameter brittle materials subjected to high strain rate. J Mater Civil Eng ASCE, 2002, 14(3):262–9.

[18] Li XB, Lok TS, Zhao J, et al. Oscillation elimination in the Hopkinson bar apparatus and resultant complete dynamic stress–strain curves for rocks. Int J Rock Mech Min Sci, 2000, 37(7):1055–60.

[19] Li XB, Lok TS, Zhao J. Dynamic characteristics of granite subjected to intermediate loading rate. Rock Mech Rock Eng, 2005, 38(1):21–39.

[20] Wang YF, Zheng XJ, Wang LP, et al.A similar test system with complete plane strain and applicable gradient stress: China, CN20141000 1118.6 [P]. 2014-04-30.

[21] Jin JF, Chang JR,Y , et al. A loading experimental method and apparatus for axial asymptotic static gradient stress: China,CN201610 073926.2[P]. 2016-06-22.

[22] Jin JF,Zhang R,Wang XB, et al. Development of a rock gradient stress loading test device and its primary application.Chinese Journal of Rock Mechanics and Engineering, 2020, 39(08): 1547-1559.

[23] Huang HJ, Wang JP, Mao YJ, et al. Influence of pretightening force of explosive bolts on impulse response. Journal of Vibration and Shock, 2015, 34(16):166-169.

[24] Liu SH, Mao DB, Qi HX, et al. Stress wave propagation mechanism and energy consumption of combined coal and rock under static and dynamic loading. ournal of China Coal Society, 2014, 39(S1):15-22.

[25] Wang HT, Xian XF. Study of elastic wave propagation characteristics of rocks under complex stress conditions,Journal of Chongqing University(Natural Sciences Edition, 1988, (05):52-59.

[26] Fan X, Wang MY, Shi CC. study on effects of initial stress on stress wave propagation and block movement law.Chinese Journal of Rock Mechanics and Engineering, 2009, 28(S2): 3442-3446.